Silencing Bcl-2 in models of mantle cell lymphoma is associated with decreases in cyclin D1, nuclear factor-κB, p53, bax, and p27 levels

Catherine A. Tucker,[1,5] Anita I. Kapanen,[1] Ghania Chikh,[1] Brad G. Hoffman,[2] Alastair H. Kyle,[3] Ian M. Wilson,[4,5] Dana Masin,[1] Randy D. Gascoyne,[6] Marcel Bally,[1,5] and Richard J. Klasa[1,7]

Departments of [1]Advanced Therapeutics, [2]Cancer Endocrinology, [3]Medical Biophysics, and [4]Cancer Genetics and Developmental Biology, BC Cancer Research Center; [5]Department of Pathology and Laboratory Medicine, University of British Columbia; Divisions of [6]Pathology and [7]Medical Oncology, British Columbia Cancer Agency, Vancouver, British Columbia, Canada

Abstract

Molecular mechanisms responsible for lymphoma resistance to apoptosis often involve the bcl-2 pathway. In this study, we investigated the cell signaling pathways activated in bcl-2-overexpressing human mantle cell lymphoma cell lines (JVM-2 and Z-138) that have been treated with oblimersen, a molecular gene silencing strategy that effectively suppresses bcl-2 *in vitro* and *in vivo*. Z-138 cells expressed higher levels of bcl-2 and were more sensitive to the effects of bcl-2 silencing, mediated by oblimersen or bcl-2 small interfering RNA, *in vitro*. Tumors derived following injection of Z-138 cells were sensitive to oblimersen as judged by decreases in tumor growth rate and decreases in cell proliferation (as measured by Ki-67). Immunohistochemistry and Western blot analysis of oblimersen-treated Z-138 tumors revealed a dose-dependent decrease in bcl-2 levels and an associated increase in the proapoptotic proteins caspase-3 and caspase-9. Silencing bcl-2 in Z-138 xenografts revealed an associated dose-dependent suppression of bax, a decrease in nuclear factor-κB and phospho-nuclear factor-κB, and transient loss of p53 levels. Coimmunoprecipitation studies suggest that the latter observation is mediated by an association between bcl-2 and phospho-mdm2. Bcl-2 silencing also led to p27 down-regulation and coimmunoprecipitation studies point to a role for bcl-2 in regulation of p27 localization/degradation. Bcl-2 silencing was also correlated with loss of cyclin D1a protein levels but not cyclin D1b levels. Coimmunoprecipitation studies indicate that bcl-2 may mediate its effects on cyclin D1a via interaction with p38 mitogen-activated protein kinase as well as a previously unreported interaction between bcl-2 and cyclin D1a. [Mol Cancer Ther 2008;7(4):749–58]

Received 4/28/07; revised 12/20/07; accepted 2/21/08.

Grant support: Lymphoma Research Foundation (R.D. Gascoyne and R.J. Klasa), Canadian Institutes of Health Research (M. Bally), and Academy of Finland and Cultural Foundation of Finland salary award (A.I. Kapanen).

The costs of publication of this article were defrayed in part by the payment of page charges. This article must therefore be hereby marked *advertisement* in accordance with 18 U.S.C. Section 1734 solely to indicate this fact.

Requests for reprints: Catherine A. Tucker, Department of Advanced Therapeutics, BC Cancer Research Center, Vancouver, British Columbia, Canada V5Z 1L3. Phone: 604-675-7024; Fax: 604-675-8183. E-mail: ctucker@bccrc.ca

doi:10.1158/1535-7163.MCT-07-0302

Introduction

One of the early events in the development of mantle cell lymphoma (MCL) is thought to be the t(11;14)(q13;q32) translocation where the immunoglobulin heavy-chain promoter is juxtaposed to the cyclin D1 gene leading to cyclin D1 overexpression (1). Cyclin D1 is believed to play an important role in the biology of MCL and a higher expression of cyclin D1 mRNA transcripts has been associated with an increased cell proliferation rate and is related to decreased survival (2). Gladden et al. showed that inhibition of cyclin D1 nuclear exportation, preventing cyclin D1 degradation in the cytoplasm, leads to a constitutive nuclear expression of cyclin D1 and induces lymphomagenesis in murine models (3). Furthermore, in addition to nuclear retention of cyclin D1, lymphoma onset correlated with perturbations in p53/mdm2/$p19^{Arf}$ expression and with bcl-2 overexpression, suggesting a role for these pathways in lymphoma development (3). Thus, in the context of MCL, it is important to consider deregulation of expression of genes involved in cell cycle progression (that is, cyclin D1 and p27) as well as those involved in cell survival/apoptosis [that is, bcl-2, nuclear factor-κB (NF-κB), p53, and bax].

Bcl-2 alters the activity of a variety of cell signaling proteins involved in apoptosis, proliferation, and cell survival (4–6). The frequency of bcl-2 overexpression in MCL has been shown to be as high as 97% (7). Although bcl-2 has been shown to have multiple independent functions, bcl-2 possesses no inherent enzymatic activity (6). The bcl-2 proto-oncogene encodes an intracellular membrane-associated protein that has been located in the mitochondria, endoplasmic reticulum, and nuclear membrane (4). Its proximity to the pore structures of the nuclear membrane is an ideal location for interacting with proteins as they cross the nuclear envelope (8). Thus, it has been proposed that bcl-2 can act as an adaptor or docking protein sequestering molecules to the nuclear membrane. This function of bcl-2 can result in inactivation of the

bound protein or may facilitate interactions with other proteins (8), such as proteins like Raf1 that possess kinase activity capable of altering multiple cell signaling pathways (6).

The role that overexpression of bcl-2 plays in mediating resistance to apoptosis through alteration of other cell signaling pathways, such as cyclin D1/p27, p53/mdm2, and NF-κB, is largely unknown in MCL. In this study, we focused on investigating the cell signaling pathways by which bcl-2-overexpressing cells mediate resistance to cell death using human MCL cell lines, Z-138 and JVM-2. For this purpose, a strategy that involved the silencing of bcl-2 with small interfering RNA (siRNA) or an antisense oligonucleotide against bcl-2 (oblimersen) was used. Silencing bcl-2 in Z-138 xenografts revealed an associated dose-dependent suppression of bax, a decrease in NF-κB and phospho-NF-κB, and transient loss of p53 levels. Coimmunoprecipitation studies suggest that the latter observation is mediated by an association between bcl-2 and phospho-mdm2. Bcl-2 silencing also led to p27 down-regulation and coimmunoprecipitation studies point to a role for bcl-2 in regulation of p27 localization/degradation. Bcl-2 silencing was also correlated with loss of cyclin D1 protein levels. Coimmunoprecipitation studies indicate that bcl-2 may mediate its effects on cyclin D1 via interaction with p38 mitogen-activated protein kinase (MAPK) as well as a previously unreported interaction between bcl-2 and cyclin D1.

Materials and Methods

Reagents and Cell Lines

Oblimersen (Genasense, G3139) is an 18-mer phosphorothioate oligonucleotide with a sequence complimentary to the first six codons of the human bcl-2 open reading frame (sequence 5′-TCTCCCAGCGTGCGCCAT-3′). G3622 (sequence 5′-TACCGCGTGCGACCCTCT-3′) is the reverse polarity sense control (RPO) of G3139, whereas G4126 (sequence 5′-TCTCCCAGCATGTGCCAT-3′) has a two-base mismatch (MMO) to G3139. Both antisense controls are phosphorothioated, linear, single-stranded 18-mer oligonucleotides. All of the oligonucleotides were kindly provided by Genta. Bcl-2 SMARTpool siRNA was purchased from Dharmacon.

MCL cell lines Z-138 and JVM-2, HBL-2, Granta 519, and NCEB-1; the human osteosarcoma cell line TC32 (bcl-2 negative control); and the human lymphoma cell line DoHH2 (bcl-2-positive control) were used in this study, and the source of the cell lines, their respective characterization in our laboratory, and cell culture conditions have been recently detailed in a separate publication (9).

Bcl-2 Silencing *In vitro*: Cell Transfections/Imaging

Z-138 and JVM-2 were transfected with oblimersen, RPO, or MMO (control) or bcl-2 siRNA by using the Amaxa Nucleofector (Amaxa) according to the manufacturer's protocol. Briefly, 3×10^6 cells were suspended into Amaxa nucleofection solution T (Z-138) or solution R (JVM-2) with 50 to 300 pmol/L bcl-2 siRNA (Dharmacon) or 100 to 600 nmol/L oblimersen (Genta). Cells transfected with FITC-labeled oblimersen (Becton Dickinson) were evaluated for transfection efficiency by flow cytometry and by confocal microscopy (CI, Nikon equipped with inverted microscope Eclipse TE2000E and plan APO 60.0×/1.45/0.13 oil immersion objective). Images were cropped and magnified with imaging system software CIsi version EZ-CI 3.0 (Nikon). Samples were analyzed using an EPICS Elite ESP flow cytometer (Beckman Coulter) equipped with an Enterprise 621 laser (Coherent). Bcl-2 and bax protein expression was analyzed by Western blotting. Nucleofected cells ($\sim 3 \times 10^6$) were incubated for 48 h before protein extraction and 25 μg protein/sample were separated on 12% SDS-acrylamide gel and electroblotted onto Protran nitrocellulose membranes (Whatman). For two-color detection, primary antibodies of anti-bcl-2 and anti-bax (DAKO) were incubated in Odyssey blocking buffer (Licor Biosciences) in dilutions of 1:1,000 and 1:500, respectively. Alexa 680–conjugated goat anti-rabbit (Molecular Probes) and IRDye 800–conjugated goat anti-mouse (Rockland Immunochemicals) secondary antibodies in dilutions of 1:15,000 in blocking buffer were incubated for 30 min. Bands were detected with Licor Odyssey Infrared imaging system (Licor Biosciences) and Odyssey software 1.2.

In vivo Xenograft Models and Treatment Schedules

Rag-2M mice (age 6-9 weeks) with transgenic knockout of the Rag-2 gene were maintained in the BC Cancer Agency Animal Resource Center. Exponentially growing cultured Z-138 cells ($\sim 5 \times 10^6$) were mixed with Matrigel (volume of 100 μL; Collaborative Biomedical Products) and injected s.c. into the flank of male Rag-2M mice. The effect of treatment with oblimersen was investigated and controls included treatment with saline, RPO, or MMO. All drugs were administered i.p. All treatments were initiated when tumors were palpable ($0.5 \times 0.5 \times 0.5$ mm), usually 16 to 20 days after cell inoculation. Groups of six mice were injected i.p. with oblimersen (5, 7.5, and 12.5 mg/kg) every day, excluding weekends, for a total of 14 injections. All animal studies were completed in accordance with the current guidelines of the Canadian Council of Animal Care and with the approval of the University of British Columbia Animal Care Committee.

Western Blot Analysis

The following antibodies were purchased from DAKO: anti-cyclin D1, anti-bcl-2, and anti-bax. The remaining antibodies were purchased from Cell Signaling: anti-p27, anti-NF-κB p65, anti-phospho-NF-κB p65-Ser^{536}, anti-cleaved caspase-9, and anti-p53 (7F5). These antibodies were used at dilutions of 1:100 or 1:1,000 for anti-bcl-2. Anti-tubulin (Covance) and anti-β-actin (Sigma) were used at dilutions of 1:100 and 1:10,000, respectively, and were used for standardization of protein loading. Secondary antibodies included an anti-mouse or an anti-rabbit IgG horseradish peroxidase (Promega). Bands were subsequently detected using enhanced chemiluminescence reagent from Amersham. It should be noted that the cyclin D1 antibody clone DCS-6 can detect both cyclin D1a and D1b proteins (3, 10).

Immunoprecipitation Studies

Protein A-Sepharose beads were purchased from Amersham Biosciences and equilibrated by repeated washes with 500 μL buffer D (11) with protease and protein phosphatase inhibitor cocktails (Calbiochem). The following antibodies were used: anti-cyclin D1 (DAKO and Cell Signaling), anti-bcl-2 (DAKO), anti-p27, anti-p38 MAPK, anti-phospho-p38 MAPK (Thr^{180}/Tyr^{182}), anti-phospho-GSK3α/β (Ser^{21}/Ser^{9}), and anti-phospho-mdm2 (Ser^{166}; Cell Signaling). Antibodies (5-10 μL each) were added to 100 to 200 μL of the cell lysates or tumor lysates and incubated either overnight or for 1 h at 4°C. Equilibrated protein A-Sepharose slurry (50 μL) was then added to each reaction and incubated at 37°C for 1 h. Several washes were done with buffer D and the pellets were collected and analyzed by SDS-PAGE.

Quantitative Real-time PCR

Total RNA from cell lines and tissues was isolated using Trizol reagent according to the manufacturer's protocols (Invitrogen). Triplicate cDNA were synthesized using 1 μg total RNA with SuperScript III (Invitrogen). Bcl-2 and porphobilinogen deaminase primers and probes were purchased from Applied Biosystems. Probes used included bcl-2 (5′-CTGAACCGGCACCTGCACACCTG-3′) and porphobilinogen deaminase (5′-CATCTTTGGGCTGTTTTCTTCCGCC-3′). All probes were labeled with the following fluorescent markers (VIC or FAM at the 5′-end and TAMRA at the 3′-end). For PCR, 1 μL cDNA was incubated with 2× Universal PCR Master Mix (Applied Biosystems), 12.5 pmol bcl-2 primer, 15.0 pmol porphobilinogen deaminase primer, and 10 pmol bcl-2 and porphobilinogen deaminase Taqman probes to a final volume of 25 μL. Analysis of mRNA expression was carried out using the ABI Prism 7500 Sequence detection system. All samples were done in triplicate.

Sequencing of TP53 Exons 5 to 8

Genomic DNA was isolated from Z-138 cells by proteinase K digestion and phenol extraction. Exon-specific PCR was done using primers that amplify exons 5 to 8 of TP53 (exon 5: TGTTCACTTGTGCCCTGACT and CAGCCCTGTCGTCTCTCCAG, exon 6: GCCTCTGATTCCTCACTGAT and TTAACCCCTCCTCCCAGAGA, exon7: ACGGGCCTCATCTTGGGCCT and TGTGCAGGGTGGCAAGTGGC, and exon 8: TAAATGGGACAGGTAGGACC and TCCACCGCTTCTTGTCCTGC-3′; ref. 12). PCR products were isolated from 1.5% agarose gels using the QiaQuick Gel Extraction Kit (Qiagen) and used for direct sequencing. Nucleotide sequences were compared against consensus exon sequences in the human genome sequence assembly at http://genome.ucsc.edu to identify mutations.

Immunohistochemistry

Formalin-fixed tumor samples were prepared for sectioning by Takeshi Kuriata (BC Cancer Agency). For staining purposes, anti-human Ki-67 (DAKO) and anti-cleaved caspase-3 (Cell Signaling) were used at dilutions of 1:100. Methods for Ki-67 staining have been described elsewhere (13). In brief, sections to be used for Ki-67 and cleaved caspase-3 staining were rehydrated and heated in 10 mmol/L citrate buffer for 30 min. Subsequently, these sections were incubated with primary antibodies at 4°C overnight followed by the addition of biotinylated secondary antibodies against anti-mouse and anti-rabbit IgG (Vector Laboratories). Immunoreactivity was visualized with Vectastain Elite ABC Kit (Vector Laboratories) and diaminobenzidine (Sigma) as the chromagen. The microscope Leica DM L (20×/0.50 HCD PL Fluotar) was used and images were acquired with Regita 1300i CCD camera (QImaging) and imaging software Openlab 5.0.1 (Improvision).

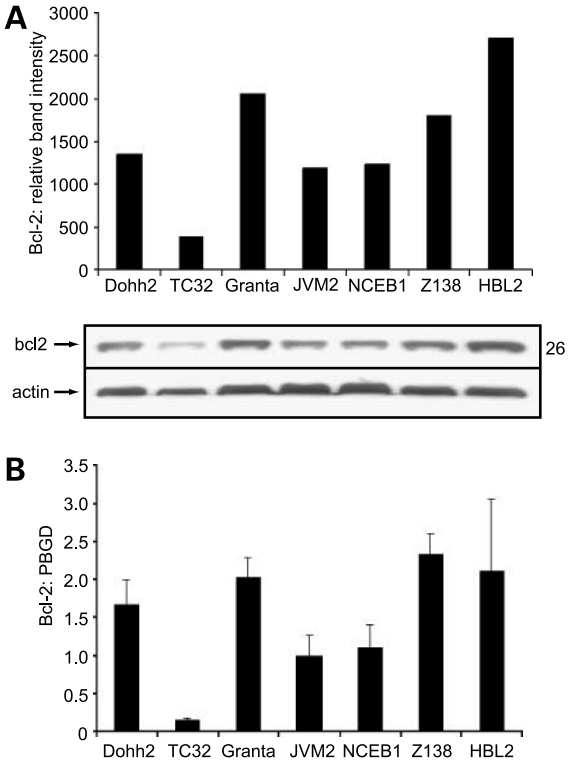

Figure 1. Bcl-2 expression in MCL cell lines is equivalent to or 2-fold higher than the DoHH2 cell line containing the bcl-2 translocation t(8;14;18) and parallels its mRNA expression levels. **A,** Western blot analysis of bcl-2 expression. DoHH2 was used as a positive control and TC32 was used as a negative control for bcl-2 expression. **B,** quantitative real-time PCR analysis of bcl-2 mRNA expression relative to the endogenous control porphobilinogen deaminase (*PBGD*).

Statistical Methods

In vivo efficacy data were analyzed using SPSS 13.0 (SPSS). The time taken for s.c. tumors to reach a size of 0.4 cm^3 was analyzed using Kaplan-Meier curves for survival analysis. This analysis allows modeling to the time event data (that is, time to reach 0.4 cm^3) in the presence of censored cases (that is, animals who never reached this endpoint because of, for example, tumor ulceration). Treatment and control groups were compared using a log-rank test. Results for quantitative real-time PCR are from triplicate samples and are presented as mean ± SD. Statistically significant differences between samples were

analyzed using two-tailed Student's t tests for unpaired samples. $P < 0.05$ was considered significant.

Results and Discussion

Overexpression of bcl-2 in MCL Lines and bcl-2 Down-Regulation *In vitro* in Z-138 and JVM-2 Cells-

All MCL cell lines examined had levels of bcl-2 protein expression either equal to or 2-fold higher than the DoHH2 cells, which were used as the bcl-2-positive control (Fig. 1A). The expression of bcl-2 mRNA followed a similar pattern to bcl-2 protein levels (Fig. 1B). Z-138 (high level of bcl-2) and JVM-2 (lowest level of bcl-2) cell lines were used for comparative purposes. In addition to the 1.8-fold higher bcl-2 expression levels, it should be noted that the Z-138 cell line exhibits an amplification of the bcl-2 gene copy number, whereas this amplification is absent in JVM-2 cells (14). In Z-138 cells, treatment with higher doses of oblimersen (600 nmol/L) and siRNA (300 pmol/L) caused a significant down-regulation of bcl-2 mRNA levels ($P < 0.025$) and led to an associated decrease in bcl-2 protein levels (Fig. 2A and B). Notably, only mRNA was significantly down-regulated in JVM-2 cells after treatment with the highest dose of siRNA (300 pmol/L; $P = 0.039$; Fig. 2B).

To determine whether differences in gene silencing could be attributed to the amount of oblimersen delivery to the cell lines, FITC-oblimersen was transfected into Z-138 and JVM-2 cells. The results summarized in Fig. 2C indicate that FITC-oblimersen delivery to Z-138 and JVM-2 cells were comparable based on confocal microscopy analysis. This result was confirmed by flow cytometry, where Z-138 (Fig. 2D, *filled triangles*) and JVM-2 cells (Fig. 2D, *open*

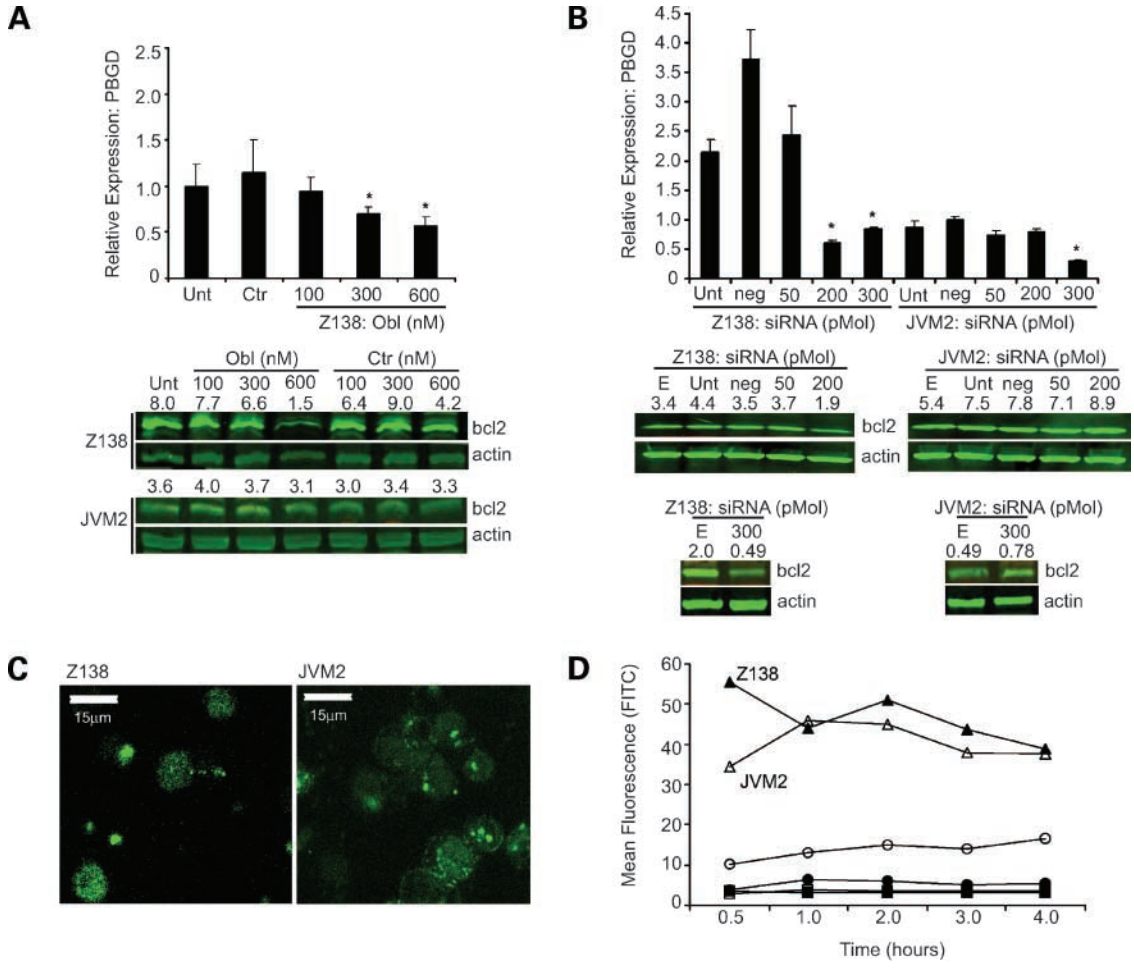

Figure 2. Bcl-2 silencing *in vitro* was greater in Z-138 cells compared with JVM-2 cells. Quantitative real-time PCR analysis and Western blot analysis (**A** and **B**) of Z-138 and JVM-2 cells left untreated (*Unt*) or treated with oblimersen (100-600 nmol/L) or control antisense oligonucleotide (*Ctr*; 100-600 nmol/L) for 48 h or treated with bcl-2 siRNA (50-300 pmol/L) or a negative siRNA control (*neg*) for 48 h. An additional control of untreated electroporated cells (*E*) was analyzed for Western blots. *Asterisk,* significant down-regulation of bcl-2. Analysis of transfection efficiency of Z-138 and JVM-2 cells following 48-h treatment with FITC-labeled oblimersen by either (**C**) confocal microscopy, images taken at ×60 oil immersion, or (**D**) flow cytometry as analyzed at different time points (1/2-4 h) after transfection. Z-138: untreated cells (■), incubation of cells with free, untransfected FITC-oblimersen (●), cells transfected with FITC-oblimersen (▲); JVM-2: untreated cells (□), free (○), transfected (Δ). Full-length gels are presented in Supplementary Fig. S1.

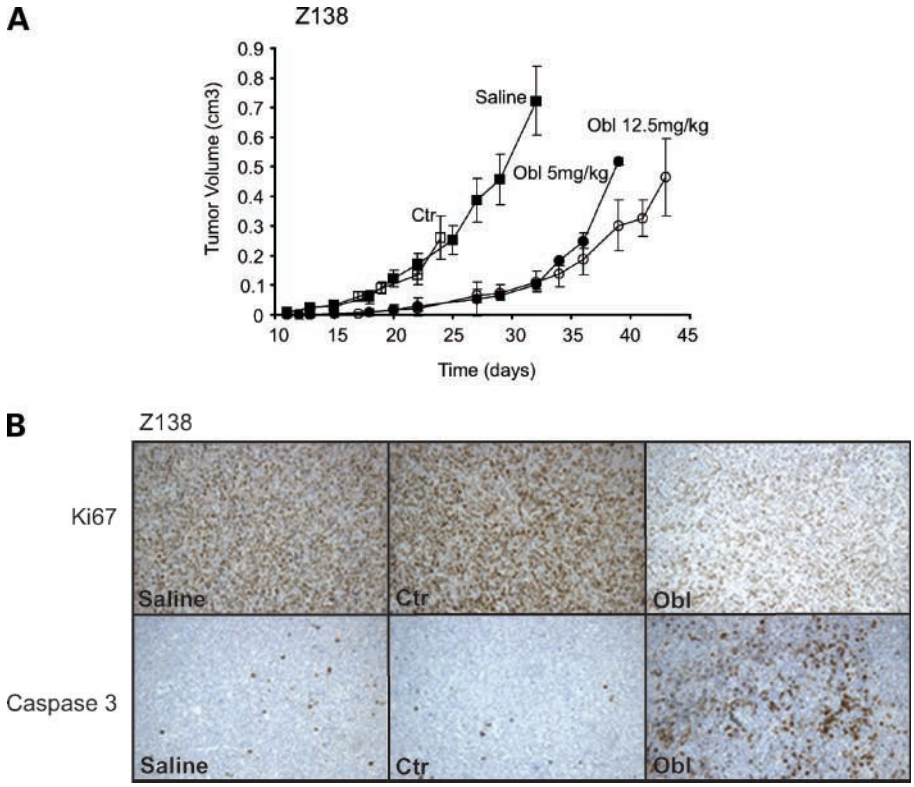

Figure 3. Z-138 xenografts exhibit a significant tumor growth delay following treatment with oblimersen. Tumor growth delay in Z-138 xenografts is associated with a marked decrease in proliferation and an associated increase in apoptosis. **A,** growth curves for Z-138 xenografts after treatment with oblimersen (5 and 12.5 mg/kg). **B,** immunohistochemistry analysis for Z-138 xenografts: Ki-67 and caspase-3 staining of tumor tissue at day 7 of treatment with either saline, control antisense oligonucleotide, or oblimersen (12.5 mg/kg). Images were taken at ×20 magnification.

triangles) transfected with FITC-oblimersen exhibited comparable uptake. Although differences in the mean fluorescence of cells were noted at 30 min after transfection, indicating that Z-138 cells had higher levels of cell associated oblimersen, these differences were not sustained. These data would indicate that differences in bcl-2 silencing could not be attributed to differences in FITC-oblimersen transfection. Z-138 cells proliferate more rapidly than JVM-2 cells (9) and it is possible that a more rapid rate of bcl-2 mRNA and protein turnover may confer a greater sensitivity to treatments targeting mRNA degradation and subsequently loss of protein levels.

Oblimersen Treatment in Z-138 Xenografts Engenders Tumor Growth Delays and Correlates to Reduced Proliferation and Apoptosis Induction

Treatment with oblimersen caused a significant tumor growth delay in animals bearing Z-138 tumors. This was observed after treatment with doses of 5 and 12.5 mg/kg oblimersen (Fig. 3A). Using time to reach a tumor volume of 0.4 cm^3 as an endpoint defining survival, a statistical analysis of the resultant Kaplan-Meir indicated that the antitumor activity of oblimersen administered at these doses was highly significant ($P < 0.0005$).

There remains some controversy over the mechanism of activity driving the therapeutic effects of oblimersen *in vivo* (15). As suggested by others, bcl-2 suppression may be the result of indirect effects (16), but these indirect effects vary depending on the system analyzed and with the appropriate controls these indirect effects can be accounted for. The antisense sequence and control sequences (RPO and MMO) used in the studies summarized here all contain an immune-activating CpG motif that could stimulate NK functions in the Rag-2M mice; however, only oblimersen was capable of inducing therapeutic effects. Previous studies from our laboratory also indicate that the therapeutic activity of oblimersen was maintained in mice that lack NK function (17); in addition, recent studies from our laboratory indicate that MCL has a novel mechanism of excluding immune cells from the tumor microenvironment;[8] thus, there is little doubt from our perspective that part of the therapeutic action of oblimersen is due to bcl-2 suppression. As indicated previously, an objective of this study was to determine how MCL cell lines respond under conditions where bcl-2 is suppressed. Because Z-138 cells exhibited sensitivity to oblimersen treatment both *in vitro* and *in vivo*, we chose this model for subsequent studies. It should be noted that the results obtained in the subsequent studies are from representative samples; however, studies were completed using a minimum of four to six animals per group.

In Z-138 xenografts, the effects of oblimersen treatment on proliferation and apoptosis was examined on day 7 after treatment initiation. As shown in Fig. 3B (*top*), treatment with oblimersen (12.5 mg/kg) led to a decrease in

[8] C.A. Tucker, A.H. Kyle, B.G. Hoffman, et al. Abnormal expression of soluble and membrane bound Fas ligand in mantle cell lymphoma: potential for resistance to Fas-mediated cell death and immune evasion. In preparation.

proliferation rates as measured by a substantial decrease in Ki-67 staining. An increase in apoptosis was also apparent as shown by the presence of cleaved caspase-3 when compared with tumors from animals treated with saline or control antisense sequence (Fig. 3B, *bottom*). Western blot analysis was used to assess whether oblimersen treatment of Z-138 tumor-bearing mice was associated with bcl-2 suppression and the results (summarized in Fig. 4A) clearly show a dose-dependent down-regulation of bcl-2. Bcl-2 protein suppression data shown in Fig. 4A were observed in tumors isolated 7 days after treatment was initiated. Previous studies have also shown maximum down-regulation of bcl-2 *in vivo* between days 5 and 7 after treatment was initiated and a return to normal levels of bcl-2 expression after day 7 despite continued treatment with oblimersen (15).

Thus, this model is an interesting one to begin to question how MCL cells are compensating in response to oblimersen engendered decreases in bcl-2 levels. For example, in MCL, overexpression of bcl-2 is associated with a decrease in expression of apoptotic effectors, such as caspase-9 (18). For this reason, the effect of bcl-2 silencing on caspase-9 levels was evaluated. The results summarized in Fig. 4B show that bcl-2 silencing *in vivo* with a 12.5 mg/kg oblimersen dose led to a time-dependent increase in caspase-9 protein expression.

Another compensating mechanism known to be associated with bcl-2 expression concerns increased expression of the proapoptotic protein bax (19). However, as shown in Fig. 4B, Z-138 tumors from mice treated with 12.5 mg/kg oblimersen exhibited a time-dependent decrease in bax levels. In addition, decreased bax levels were also observed when the Z-138 cells were treated *in vitro* with oblimersen (Fig. 4B). The biological significance for the observed decreases in bax protein expression following bcl-2 silencing is not known; however, this may not be a direct effect of bcl-2 but rather an indirect one following down-regulation of other proteins. Because p53 is involved in bax transcriptional regulation (20), it is reasonable to speculate that bax down-regulation may occur as a result of p53 down-regulation and this possibility was addressed in the studies described below.

Silencing bcl-2 in Z-138 Xenografts Led to Down-Regulation of p53 Expression and Immunoprecipitation Studies Show That bcl-2 Coprecipitates Phospho-mdm2

The results summarized in Fig. 4C indicate that bcl-2 down-regulation is associated with suppression of p53. Suppression is observed in tumors isolated from mice treated with 5 and 12.5 mg/kg oblimersen and the expression returns to control levels within 7 days. It is known that bcl-2 can interact directly with p53 in conjunction with c-myc to prevent p53 nuclear localization leading to abrogation of the apoptotic effects of p53 (5). In addition, bcl-2 and p53 complexes are important regulators of apoptosis at the mitochondrial membrane (21). However, the reason why bcl-2 suppression is associated with decreased expression of p53 is not clear and this phenomenon has also been observed in breast cancer (22). One possibility is that bcl-2 silencing leading to down-regulation of p53 may be the result of p53 nuclear localization followed by p53 transcriptional regulation of its own inhibitor, mdm2. It is well established that p53 transcriptionally activates the mdm2 gene, and the mdm2 protein in turn regulates p53 levels by binding to p53, which in turn triggers proteasome-mediated degradation (23).

Another possibility that was explored in this study is that bcl-2 could have a direct effect on mdm2. Recently, a tissue microarray study on tumor samples obtained from MCL patients indicated that expression of bcl-2 was associated with a down-regulation of mdm2 (7). Thus, interactions between bcl-2 and mdm2 both *in vitro* and *in vivo* were

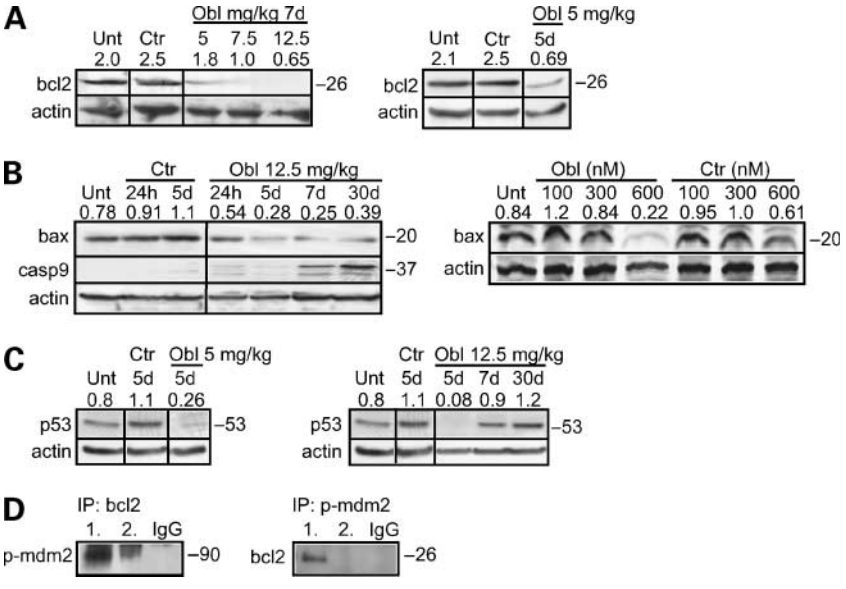

Figure 4. Oblimersen treatment in Z-138 xenografts leads to a dose-dependent down-regulation of bcl-2 as well as an associated up-regulation in caspase-9 and down-regulation of bax. Silencing bcl-2 *in vivo* also leads to a loss in p53 expression and bcl-2 coprecipitates with phospho-mdm2. Western blot analysis of Z-138 tumors after treatment with either saline, control antisense oligonucleotide, or oblimersen at doses of (5, 7.5, and 12.5 mg/kg) for (**A**) bcl-2 levels or (**B**) caspase-9 and bax levels. *In vitro* analysis of bax expression by Western blot analysis of Z-138 cells left untreated or treated with oblimersen (100-600 nmol/L) or control antisense oligonucleotide (100-600 nmol/L) for 48 h. **C,** Western blot analysis for p53 expression of Z-138 tumors after treatment with either saline, control antisense oligonucleotide, or oblimersen (5 and 12.5 mg/kg). **D,** coimmunoprecipitation (*IP*) studies of bcl-2 and mdm2. *Lane 1,* IP for Z-138 tumor lysate; *lane 2,* IP for Z-138 cell lysate. Results obtained are from representative samples; however, studies were completed using a minimum of four to six animals. Full-length gels are presented in Supplementary Fig. S1.

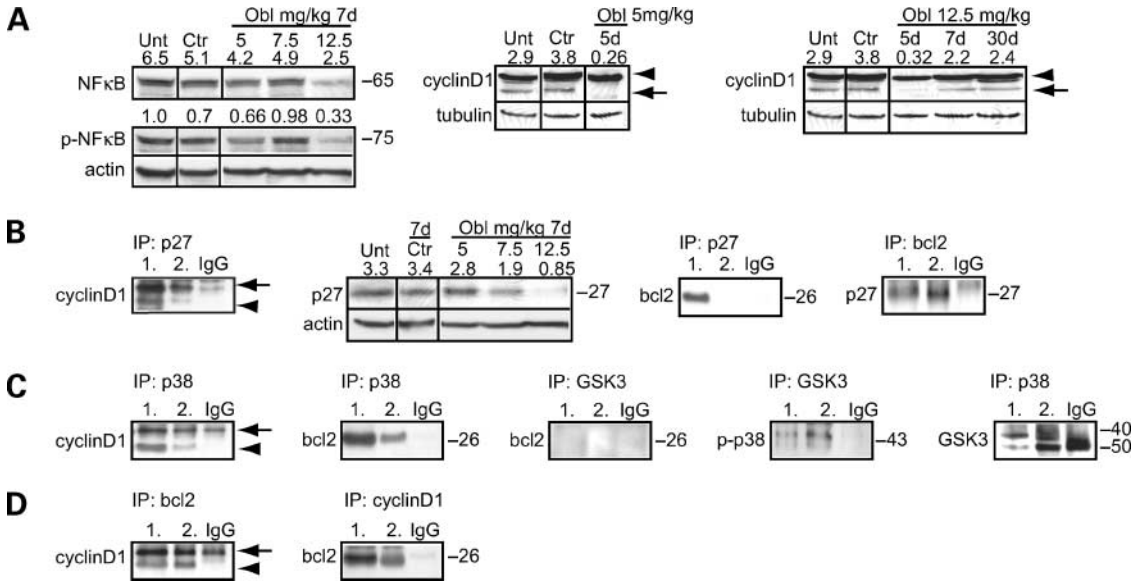

Figure 5. Oblimersen treatment in Z-138 xenografts leads to loss of expression of NF-κB and its phosphorylated form, p27 and cyclin D1a. Coimmunoprecipitation studies indicate that bcl-2 is coprecipitated with p27, p38 MAPK, and cyclin D1a and D1b, but not GSK3β, which coprecipitates with p38 MAPK. Western blot analysis of Z-138 tumors after treatment with either saline, control antisense oligonucleotide, or oblimersen at doses of (5, 7.5, and 12.5 mg/kg) for (**A**) NF-κB, cyclin D1a, and cyclin D1b (*long arrow,* cyclin D1a; *short arrow,* cyclin D1b protein) and (**B**) p27 levels. Coimmunoprecipitation studies for (**B**) IP for p27 and cyclin D1, IP for p27 and bcl-2, and IP for bcl-2 and p27; (**C**) IP for p38 MAPK and cyclin D1, IP for p38 MAPK and bcl-2, IP for GSK3 and bcl-2, IP for GSK3 and phospho-p38 MAPK, and IP for p38 MAPK and GSK3; and (**D**) IP for bcl-2 and cyclin D1 and IP for cyclin D1 and bcl-2. *Lane 1,* IP for Z-138 tumor lysate; *lane 2,* IP for Z-138 cell lysate. Results obtained are from representative samples; however, studies were completed using a minimum of four to six animals. Full-length gels are presented in Supplementary Fig. S1.

assessed using coimmunoprecipitation strategies. The results summarized in Fig. 4D confirmed that bcl-2 can be coprecipitated with phospho- mdm2. These results indicate a role for bcl-2 in the degradation/localization of p53 expression mediated by mdm2, perhaps by sequestering/inactivating the active phosphorylated form of mdm2 and preventing its translocation into the nucleus or preventing mdm2-mediated degradation of p53 in the cytoplasm. mdm2 can target p53 protein for degradation in the cytoplasm but can also inhibit p53 transcriptional activity in the nucleus once mdm2 is activated by phosphorylation at Ser^{166} and Ser^{186} by the protein-serine/threonine kinase Akt/protein kinase B (24).

Although these observations would explain why bcl-2 silencing could lead to p53 down-regulation, the biological significance of these events still needs to be elucidated. p53 overexpression is usually associated with TP53 mutations and TP53 mutations are correlated with a more aggressive blastoid variant in MCL (25, 26). Therefore, TP53 exons 5 to 8 of the cell line Z-138 were sequenced and no mutations were found. The sequestration of wild-type p53 in the cytoplasm can greatly alter its effects on inducing apoptosis (5). Therefore, it is plausible that bcl-2 plays a role in the localization/degradation of wild-type p53, which would greatly alter its effects on apoptosis/cell survival and needs to be further elucidated. In addition, p53 has a complex interaction with different components of the NF-κB cell signaling pathways and p53 can act in conjunction with NF-κB on the cyclin D1 promoter to regulate cyclin D1 expression (27). As such, the effects of bcl-2 silencing on these molecules were explored and are discussed below.

Silencing bcl-2 in Z-138 Xenografts Engenders a Decrease in NF-κB and Phospho-NF-κB, p27, and Cyclin D1a

NF-κB has been shown to be constitutively active in MCL (28). Interestingly, studies on tissue microarray samples in MCL indicate that NF-κB activation (as measured by IκBα phosphorylation) was significantly associated with bcl-2 expression (7). The Western blot analysis from oblimersen-treated Z-138 tumor-bearing animals (Fig. 5A) shows that treatment resulted in down-regulation of NF-κB-p65 and its phosphorylated form. These data could be explained by implicating a role for bcl-2 expression in maintaining the constitutive activation of NF-κB seen in MCL. Other studies, for example, have shown that bcl-2 through its BH4 domain can interact with the kinase Raf1 (29, 30). Bcl-2 interaction with this kinase can lead to downstream activation of extracellular signal-regulated kinase 1/2, which in turn induces degradation of IκBα (6, 31). This contributes to the constitutive activation of NF-κB (6, 31). NF-κB is a well-established transcription factor that regulates the expression of many important genes involved in cell survival and differentiation, including the promotion of both bcl-2 (32) and cyclin D1 expression (33).

Because the role of bcl-2 in mediating control over cyclin D1 expression in MCL has not been explored previously, the tumors obtained from mice treated with oblimersen were assessed for cyclin D1 expression as well as

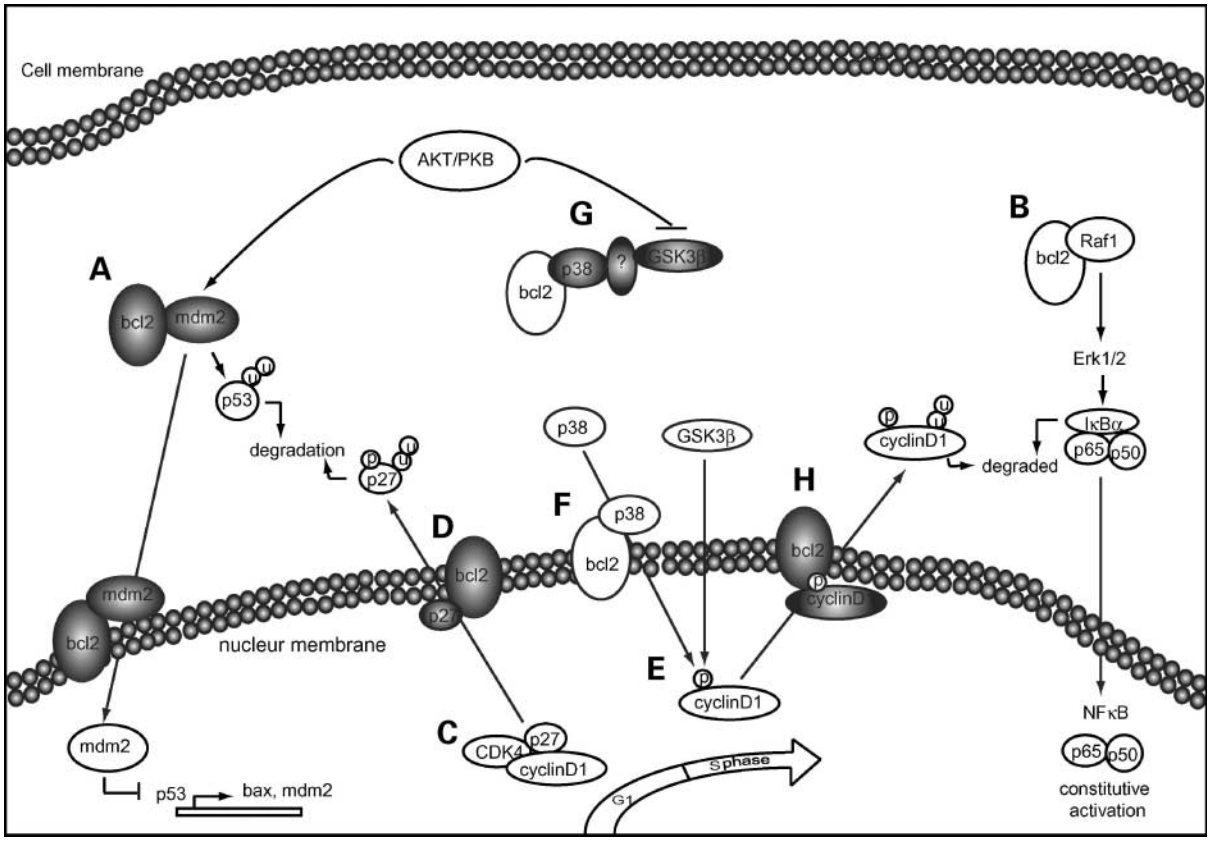

Figure 6. Proposed model of altered cell signaling events following bcl-2 silencing in an *in vivo* model of MCL. *Shaded areas,* proposed interactions based on the coimmunoprecipitation studies; *white areas,* previously known interactions/cell signaling pathways. **A,** proposed interaction between bcl-2 and mdm2 leading to p53 regulation. **B,** known interaction between bcl-2 and Raf1 leading to NF-κB constitutive activation. **C,** p27 is sequestered by cyclin D1/CDK4 in MCL. **D,** proposed interaction between bcl-2 and p27 potentially altering p27 localization/degradation. **E,** known interaction between cyclin D1 and either p38 MAPK or GSK3β leading to cyclin D1 phosphorylation/degradation. **F,** known interaction between bcl-2 and p38 MAPK, which may lead to maintenance of cyclin D1a expression. **G,** proposed interaction between p38 MAPK and GSK3β possibly mediated through another scaffold protein. **H,** proposed interaction between cyclin D1a and bcl-2 possibly preventing cyclin D1a exportation from the nucleus/degradation.

expression of a well-known cell cycle inhibitor, p27. It should be noted, however, that analysis of cyclin D1 expression in MCL is complex. The cyclin D1 gene is ~15 kb and has 5 exons. Two major cyclin D1 mRNA transcripts have been identified and termed cyclin D1a and D1b (10, 34). Cyclin D1a transcripts were the first to be discovered and are typically more abundant than cyclin D1b transcripts; however, cyclin D1b transcripts appear to be more predominant when the t(11;14) is present (10). Cyclin D1b is an alternatively spliced cyclin D1 transcript that arises due to a gene polymorphism (A/G) at codon 241 and lacks exon 5 (35). Cyclin D1b proteins lack an important phosphorylation site (Thr^{286}) targeting cyclin D1 exportation from the nucleus and its subsequent degradation during the S phase of the cell cycle (34). Results from Gladden et al. indicate that cyclin D1b may be important in the early transformation events seen in MCL, but Wiestner et al. have recently shown that cyclin D1a transcripts are important for events that lead to a more highly proliferative, aggressive MCL disease (3, 36). For this reason, the effects of oblimersen treatment on the levels of cyclin D1a and D1b were assessed. The results indicate that, following bcl-2 silencing *in vivo*, there was a concomitant decrease in cyclin D1a protein levels (Fig. 5A, *long arrow*). Importantly, cyclin D1b protein levels were not down-regulated by oblimersen treatment (Fig. 5A, *short arrow*).

It is unclear at this stage if cyclin D1a and D1b are under the same transcriptional regulation. In general, cyclin D1a enters the nucleus where it accumulates and assembles with CDK4 during G_1 phase of the cell cycle. This event occurs in response to Ras-associated signaling pathways triggered by mitogens (37). Once in the nucleus, association with p27 can further promote the assembly/stabilization of cyclin D1/CDK4 complexes (38). When p27 is complexed with cyclin D1/CDK4, its inhibitory functions on other cell cycle effectors are prevented leading to their activation (38). Interestingly, MCL was found to be atypical compared with other lymphomas, as p27 expression did not have an inverse relationship with cell proliferation (39). This latter observation is what prompted the discovery in MCL that p27 is highly sequestered by cyclin D1/CDK4 complexes due to an overabundance of cyclin D1 (40). Thus, it was of

interest to determine if p27 was complexed with cyclin D1 in our study. As summarized in Fig. 5B, coimmunoprecipitations confirmed that p27 and cyclin D1a and D1b were coprecipitated. Because cyclin D1 association with p27 is thought to prevent p27 degradation in MCL (40), it was also important to determine if bcl-2 silencing, through cyclin D1a down-regulation, may mediate a decrease in p27 protein levels.

To address this, Z-138 tumors from oblimersen-treated animals were assessed for p27 by Western blot analysis. The results summarized in Fig. 5B show that treatment with oblimersen was associated with a dose-dependent reduction in p27 levels. Other investigators, studying breast cancer, have also noted a correlation between loss of bcl-2 protein expression and loss of p27 expression (22), but the data presented here are the first to show that this effect on p27 may be mediated through cyclin D1a down-regulation. The possibility of a direct interaction between bcl-2 and p27 was also evaluated and the coimmunoprecipitation studies shown in Fig. 5B show that p27 and bcl-2 coprecipitate, an interaction that has not been noted previously. This indicates the possibility that bcl-2 located near the nuclear pores could play a more direct role in p27 localization/degradation.

Bcl-2 Overexpression Leading to Maintenance of Cyclin D1a Expression May Occur through p38 MAPK-Mediated Signaling Pathways

To determine how bcl-2 influences cyclin D1a protein levels the role of p38 MAPK was considered. Cyclin D1a and D1b differ in that cyclin D1b has lost exon 5, leading to a protein that cannot be phosphorylated at Thr^{286}, hence exported from the nucleus and degraded (34). GSK3β has been shown to be the main protein involved in phosphorylating cyclin D1 at Thr^{286} (37). Recently, in a MCL *in vitro* model, the stress-induced protein-serine/threonine kinase p38 MAPK has also been shown to directly bind and phosphorylate cyclin D1 at Thr^{286} leading to its degradation (41). Thus, p38 MAPK acts as a dual-negative regulator of cyclin D1a expression as it also inhibits cyclin D1 transcription (41). Hence, p38 MAPK is acting in opposition of the Ras signaling pathways, which enhances cyclin D1 transcription and decreases cyclin D1 degradation by inducing Akt/protein kinase B to phosphorylate GSK3β on Ser^{9} rendering it inactive (37). As p38 MAPK plays a major role in both negatively regulating cyclin D1 mRNA and protein levels and bcl-2 has recently been shown to directly interact with p38 MAPK (42), interactions between p38 MAPK/cyclin D1/bcl-2 were assessed using coimmunoprecipitation methods and these data are summarized in Fig. 5C. An assessment of cultured Z-138 cells, as well as Z-138 tumors, clearly show that p38 MAPK and cyclin D1a and D1b can be coprecipitated. Furthermore, bcl-2 and p38 MAPK were also coprecipitated (Fig. 5C). These data indicate that in MCL bcl-2 may influence cyclin D1a expression levels through an interaction with p38 MAPK.

It is also possible that bcl-2 interaction with GSK3β could interfere with its ability to phosphorylate Thr^{286} on cyclin D1a. To assess this possibility, coimmunoprecipitations were completed and the results (Fig. 5C) indicate that GSK3β does not coprecipitate with bcl-2 in Z-138 cells or in Z-138 tumors. We then sought to determine if bcl-2 may influence GSK3β indirectly through its interaction with p38 MAPK. Interestingly, GSK3β coprecipitated p38 MAPK (Fig. 5C). An interaction between bcl-2 and p38 MAPK leading to regulation of GSK3β may explain why oblimersen-mediated bcl-2 silencing is only able to influence the expression levels of cyclin D1a and not cyclin D1b.

In addition, the possibility of a direct interaction of bcl-2 and cyclin D1 (a and b forms) was not excluded. The results of these coimmunoprecipitation studies indicate that bcl-2 can coprecipitate cyclin D1a and D1b and vice versa (Fig. 5D). Hence, it is possible that bcl-2 may act directly on cyclin D1a by preventing its exportation from the nucleus and hence its degradation. The interesting possibility that GSK3β/cyclin D1/p38 MAPK/bcl-2 exist as a single signalosome or part of a signalosome cannot be excluded. The preliminary evidence provided here supports a role for bcl-2 in maintaining cyclin D1a expression. A more detailed analysis will have to be carried out to determine the exact nature of these interactions and the biological outcomes associated with these interactions.

In summary, although bcl-2 possesses no inherent enzymatic activity, a growing body of evidence supports a strong role for bcl-2 as a docking protein, whereas bcl-2 can alter cell signaling pathways by sequestering/inactivating molecules that engender kinase activity, such as Raf1 and p38 MAPK, or preventing proteins from crossing membranes, such as the nucleus. In light of this knowledge, it is shown here for the first time that bcl-2 silencing in MCL can lead to alteration of several important cell signaling pathways and these pleiotropic effects have been summarized in the model presented in Fig. 6. Although at present these studies provide strong preliminary results of the cell signaling pathways affected by bcl-2 overexpression in MCL, future studies are needed to delineate the exact nature of the interaction of bcl-2 with these proteins and to determine the eventual biological outcomes of these events in MCL.

Acknowledgments

We thank Dr. Martin J.S. Dyer (University of Leicester) for kindly providing the MCL cell lines, Dr. Poul Sorensen for kindly providing the TC32 osteosarcoma cell line, Dr. Zeev Estrov for providing the Z-138 cell line, Bogard Zavaglia for help with the coimmunoprecipitation studies, and John Fee for help with the confocal microscopy studies.

References

1. Swerdlow SH, Williams ME. From centrocytic to mantle cell lymphoma: a clinicopathologic and molecular review of 3 decades. Hum Pathol 2002; 33:7 – 20.

2. Rosenwald A, Wright G, Wiestner A, et al. The proliferation gene expression signature is a quantitative integrator of oncogenic events that predicts survival in mantle cell lymphoma. Cancer Cell 2003;3:185 – 97.

3. Gladden AB, Woolery R, Aggarwal P, Wasik MA, Diehl JA. Expression of constitutively nuclear cyclin D1 in murine lymphocytes induces B-cell lymphoma. Oncogene 2006;25:998 – 1007.

4. Borner C. The Bcl-2 protein family: sensors and checkpoints for life-or-death decisions. Mol Immunol 2003;39:615 – 47.

5. Ryan JJ, Prochownik E, Gottlieb CA, et al. c-myc and bcl-2 modulate

p53 function by altering p53 subcellular trafficking during the cell cycle. Proc Natl Acad Sci U S A 1994;91:5878 – 82.

6. Jang JH, Surh YJ. Bcl-2 attenuation of oxidative cell death is associated with up-regulation of γ-glutamylcysteine ligase via constitutive NF-κB activation. J Biol Chem 2004;279:38779 – 86.

7. Tracey L, Perez-Rosado A, Artiga MJ, et al. Expression of the NF-κB targets BCL2 and BIRC5/survivin characterizes small B-cell and aggressive B-cell lymphomas, respectively. J Pathol 2005;206:123 – 34.

8. Reed JC. Double identity for proteins of the bcl-2 family. Nature 1997; 387:773 – 6.

9. Tucker CA, Bebb G, Klasa RJ, et al. Four human t(11;14)(q13;q32)-containing cell lines having classic and variant features of mantle cell lymphoma. Leuk Res 2006;30:449 – 57.

10. Hosokawa Y, Joh T, Maeda Y, Arnold A, Seto M. Cyclin D1/PRAD1/BCL-1 alternative transcript [b] protein product in B-lymphoid malignancies with t(11;14)(q13;q32) translocation. Int J Cancer 1999;81:616 – 9.

11. Husein J, Lo R, Grbavec D, Stifani S. Affinity for the nuclear compartment and expression during cell differentiation implicate phosphorylated Groucho/TLE1 forms of higher molecular mass in nuclear functions. Biochem J 1996;317:523 – 31.

12. Sakai E, Tsuchida N. Most human squamous cell carcinomas in the oral cavity contain mutated p53 tumor-suppressor genes. Oncogene 1992;7:927 – 33.

13. Kurita T, Medina R, Schabel AB, et al. The activation function-1 domain of estrogen receptor α in uterine stromal cells is required for mouse but not human uterine epithelial response to estrogen. Differentiation 2005;73:313 – 22.

14. de Leeuw RJ, Davies JJ, Rosenwald A, et al. Comprehensive whole genome array CGH profiling of mantle cell lymphoma model genomes. Hum Mol Genet 2004;13:1827 – 37.

15. Lebedeva I, Stein CA. Antisense oligonucleotides: promise and reality. Annu Rev Pharmacol Toxicol 2001;41:403 – 19.

16. Castro JE, Prada CE, Aguillon RA, et al. Thymidine-phosphorothioate oligonucleotides induce activation and apoptosis of CLL cells independently of CpG motifs or BCL-2 gene interference. Leukemia 2006;20: 680 – 8.

17. Klasa RJ, Bally MB, Ng R, Goldie JH, Gascoyne RD, Wong FMP. Eradication of human non-Hodgkin's lymphoma in SCID mice by bcl-2 antisense oligonucleotides combined with low-dose cyclophosphamide. Clin Can Res 2000;6:2492 – 500.

18. Hofmann WK, de Vos S, Tsukasaki K, et al. Altered apoptosis pathways in mantle cell lymphoma detected by oligonucleotide microarray. Blood 2001;98:787 – 94.

19. Green DR. Apoptotic pathways: paper wraps stone blunt scissors. Cell 2000;102:1 – 4.

20. Miyashita T, Reed JC. Tumor suppressor p53 is a direct transcriptional activator of the human bax gene. Cell 1995;80:293 – 9.

21. Deng X, Gao F, Flagg T, Anderson J, May WS. Bcl-2's flexible loop domain regulates p53 binding and survival. Mol Cell Biol 2006;26: 4421 – 34.

22. Tsutsui S, Yasuda K, Suzuki K, et al. Bcl-2 protein expression is associated with p27 and p53 protein expressions and MIB-1 counts in breast cancer. BMC Cancer 2006;6:187.

23. Wu X, Bayle JH, Olson D, Levine AJ. The p53-mdm-2 autoregulatory feedback loop. Genes Dev 1993;7:1126 – 32.

24. Mayo LD, Donner DB. A phosphatidylinositol 3-kinase/Akt pathway promotes translocation of mdm-2 from the cytoplasm to the nucleus. Proc Natl Acad Sci U S A 2001;98:11598 – 603.

25. Khoury JD, Medeiros LJ, Rassidakis GZ, McDonnell TJ, Abruzzo LV, Lai R. Expression of mcl-1 in mantle cell lymphoma is associated with high-grade morphology, a high proliferative state, and p53 overexpression. J Pathol 2003;199:90 – 7.

26. Greiner TC, Moynihan MJ, Chan WC, et al. p53 mutations in mantle cell lymphoma are associated with variant cytology and predict a poor prognosis. Blood 1996;87:4302 – 10.

27. Rocha S, Martin AM, Meek DW, Perkins ND. p53 represses cyclin D1 transcription through down regulation of bcl-3 and inducing increased association of the p52 NF-κB subunit with histone deacetylase 1. Mol Cell Biol 2003;23:4713 – 27.

28. Pham LV, Tamayo AT, Yoshimura LC, Lo P, Ford RJ. Inhibition of constitutive NF-κB activation in mantle cell lymphoma B cells leads to induction of cell cycle arrest and apoptosis. J Immunol 2003;171:88 – 95.

29. Wang H, Rapp UR, Reed JC. Bcl-2 targets the protein kinase raf-1 to mitochondria. Cell 1996;87:629 – 38.

30. Gary-Gouy H, Sainz-Perez A, Bismuth G, Ghadiri A, Perrino BA, Dalloul A. Cyclosporin-A inhibits ERK phosphorylation in B cells by modulating the binding of raf protein to bcl-2. Biochem Biophys Res Commun 2006;344:134 – 9.

31. Feinman R, Koury J, Thames M, Barlogie B, Epstein J, Siegel DS. Role of NF-κB in the rescue of multiple myeloma cells from glucocorticoid-induced apoptosis by bcl-2. Blood 1999;93:3044 – 52.

32. Kurland JF, Kodym R, Story MD, Spurgers KB, McDonnell TJ, Raymond EM. NF-κB1 (p50) homodimers contribute to transcription of the bcl-2 oncogene. J Biol Chem 2001;276:45380 – 6.

33. Guttridge DC, Albanese C, Reuther JY, Pestell RG, Baldwin AS. NF-κB controls cell growth and differentiation through transcriptional regulation of cyclin D1. Mol Cell Biol 1999;19:5785 – 99.

34. Lu F, Gladden AB, Diehl JA. An alternatively spliced cyclin D1 isoform, cyclin D1b, is a nuclear oncogene. Cancer Res 2003;63: 7056 – 61.

35. Howe D, Lynas C. The cyclin D1 alternative transcripts [a] and [b] are expressed in normal and malignant lymphocytes and their relative levels are influenced by the polymorphism at codon 241. Haematologica 2001; 86:563 – 9.

36. Wiestner A, Tehrani M, Chiorazzi M, et al. Point mutations and genomic deletions in CCND1 create stable truncated mRNAs that are associated with increased proliferation rate and shorter survival. Blood 2007;109:4599 – 606.

37. Alt JR, Cleveland JL, Hannink M, Diehl A. Phosphorylation-dependent regulation of cyclin D1 nuclear export and cyclin D1-dependent cellular transformation. Genes Dev 2000;14:3102 – 14.

38. Sherr CJ, Roberts JM. CDK inhibitors: positive and negative regulators of G_1-phase progression. Genes Dev 1999;13:1501 – 12.

39. Quintanilla-Martinez L, Thieblemont C, Fend F, et al. Mantle cell lymphomas lack expression of p27kip1 a cyclin-dependent kinase inhibitor. Am J Pathol 1998;153:175 – 82.

40. Quintanilla-Martinez L, Davies-Hill T, Fend F, et al. Sequestration of p27kip1 protein by cyclin D1 in typical and blastic variants of mantle cell lymphoma (MCL): implications for pathogenesis. Blood 2003;101: 3181 – 7.

41. Casanovas O, Miro F, Estanyol JM, Itarte E, Agell N, Bachs O. Osmotic stress regulates the stability of cyclin D1 in a p38sapk2-dependent manner. J Biol Chem 2000;275:35091 – 7.

42. Torcia M, De Chiara G, Nencioni L, et al. Nerve growth factor inhibits apoptosis in memory B lymphocytes via inactivation of p38 MAPK, prevention of bcl-2 phosphorylation, and cytochrome *c* release. J Biol Chem 2001;276:39027 – 36.